

Multi-RIS Communication Systems: Asymptotic analysis of best RIS selection for i.n.i.d. Random Variables using Extreme Value Theory

Srinivas Sagar and Sheetal Kalyani

Abstract

This paper investigates the performance of multiple reconfigurable intelligent surfaces (multi-RIS) communication systems where the RIS link with the highest signal-to-noise- ratio (SNR) is selected at the destination. In practice, all the RISs will not have the same number of reflecting elements. Hence, selecting the RIS link with the highest SNR will involve characterizing the distribution of the maximum of independent, non-identically distributed (i.n.i.d.) SNR random variables (RVs). Using extreme value theory (EVT), we derive the asymptotic distribution of the normalized maximum of i.n.i.d. non-central chi-square (NCCS) distributed SNR RVs with one degree of freedom (d.o.f) and then extend the results for k -th order statistics. Using these asymptotic results, the outage capacity and average throughput expressions are derived for the multi-RIS system. The results for independent and identically distributed (i.i.d.) SNR RVs are then derived as a special case of i.n.i.d. RVs. All the derivations are validated through extensive Monte Carlo simulations, and their utility is discussed.

Index Terms

reflecting intelligent surfaces, extreme value theory, non-central chi-square, independent, non-identically distributed random variables

The authors are with the Department of Electrical Engineering, Indian Institute of Technology Madras, India. Emails: {ee21d051@smail, skalyani@ee}.iitm.ac.in

I. INTRODUCTION

Reconfigurable intelligent surfaces (RISs) have gained significant popularity in the last few years [1]–[7]. Various applications such as beamforming [1], [8], [9], multiple input multiple output (MIMO) [4], [5], deep learning [10], unmanned aerial vehicles (UAVs) [11], simultaneous wireless information and power transfer (SWIPT) system [5], non-orthogonal multiple access (NOMA) [12], and millimeter wave (mmWave) systems [13] now use the RIS.

RIS-aided communication can be grouped into two categories: single-RIS and multi-RIS systems. Performance analysis of single-RIS communication systems is extensively studied in [1], [4], [6]–[10], [14]–[19]. To improve the system performance works like [1], [8], [9] presented single RIS communication systems in multi-antenna transmitter [1], multiuser communication [8], and SWIPT [9] to minimize the transmit power, hybrid beamforming, active and passive beamforming, respectively.

The results of [20] show that, in an RIS-aided communications system, received SNR at the destination can be modeled as non-central chi-square (NCCS) distribution with one degree of freedom (d.o.f) where the parameters $\left(\lambda = \left(\frac{N\pi}{4}\right)^2, \sigma^2 = N \left(1 - \frac{\pi^2}{16}\right)\right)$ only depend on the number of reflecting elements (N) of RIS. The authors of [21] introduced the quantitative analysis of coverage area. Here, the source communicates to the destination through a single RIS.

In a multi-RIS system, multiple RIS links are available between the source and destination along with a direct link. Works like [22]–[29] used the direct link and reflected links from all the RISs in deriving the outage probability and throughput analysis of multi-RIS systems. Authors of [22] considered the statistical characterization of exhaustive RIS-aided (transmit the RIS signal along with a direct signal) and opportunistic RIS-aided (only the best RIS along with a direct signal) systems. Multi-RIS systems are explored in several communications applications like cooperative communication [23], single cell networks with backhaul capacity [24], cooperative RIS, and opportunistic RIS methods for terahertz communication systems [27]. Also, the performance analysis of a multi-RIS system was presented in [25], [26], [28]. The authors of [29] derived outage probability expression for the UAV-NOMA-mmWave system with multiple RISs. Multi-RIS systems are also useful when no direct link is available between source and destination. Several works [30]–[33] select the RIS link, giving the highest SNR at the destination. The authors derived outage probability and throughput expressions using

opportunistic RIS selection for SISO [32] and mmWave [33] systems.

The multi-RIS system considered in [34] assumed that all the RISs would have the same number of reflecting elements leading to i.i.d. SNR links. Then, the authors used EVT to characterize the order statistics of the received SNR distribution. But in practice, the number of reflecting elements in each RIS will be different, leading to i.n.i.d. SNR RVs. The primary motivation of our paper is to characterize the order statistics of i.n.i.d NCCS RVs with one d.o.f and use that to select the best RIS among the multiple RISs.

The primary focus of EVT is the statistical characterization of extreme (maximum/minimum) values. EVT results have been extensively used in the fields of communication like multiuser diversity [35], [36], cognitive radio (CR) [37], [38], relays [37], MIMO, ultra-reliable and low-latency communication (URLLC) [39], [40], and machine learning. In most scenarios, finding the exact CDF of the maximum order statistics, i.e., $\prod_{r=1}^R F_r(\gamma)$ leads to very complicated expressions for large R . Several authors used EVT to characterize the maximum order statistic since this leads to mathematically tractable expressions. In multiuser diversity systems, throughput analysis is carried out asymptotically with the help of EVT [35], [36]. CR systems used EVT to find the limiting distribution of end-to-end SNR [37], to analyze spectrum and energy efficiency [38], and for optimum power allocation [41]. Also, in URLLC systems, EVT has been used to characterize the tail distribution of queue length [39], [40]. The works in [42], [43] presented the asymptotic distribution of maximum order statistics for i.i.d. sums of non-identical gamma RVs [42] and $\kappa - \mu$ shadow fading RVs [43] respectively.

To the best of our knowledge, while EVT has been used extensively in characterizing communication systems, the focus has been on i.i.d. RVs. Characterization of the asymptotic distribution of order statistics of i.n.i.d. RVs [44], [45] is mathematically more complicated than the characterization of i.i.d. RVs. Our work in [46] was the first to consider i.n.i.d. RVs in the context of an opportunistic relaying system with the SWIPT network. We then further derived the order statistics of i.n.i.d. Rician fading RVs [47]. From [20], we can observe that end-to-end SNR in RIS-aided communication system can be modeled as NCCS RV with one d.o.f, so we would like to characterize the order statistics of NCCS RV with one d.o.f. Given the order statistics of RVs, many applications (selection diversity, relay selection, antenna selection) in communications select the maximum order statistic for communication. Sometimes, the best selection/maximum order statistic may not be available for communication, in such scenarios, k -th best link can be selected for communication. Hence, we would also like to study the order statistics of NCCS

RV with one d.o.f to characterize the end-to-end SNR of a multi-RIS system. Now, we present the main contributions of this paper.

- 1) We present the performance analysis of a multi-RIS system with the help of EVT. Modeling the end-to-end SNR of a RIS-aided communication system as NCCS RV with one d.o.f, we first derive the asymptotic distribution of the normalized maximum of R i.n.i.d. NCCS RVs with the help of EVT. The asymptotic distribution of k -th maximum of i.n.i.d. NCCS RVs is also derived.
- 2) Assumption of the same number of reflecting elements for all the RISs gives us i.i.d. NCCS RVs. So, the asymptotic distribution of k -th order statistics for R i.i.d. NCCS RVs with one d.o.f is also derived as a special case of i.n.i.d. RVs.
- 3) Using the asymptotic distribution of maximum order statistics of SNR RV, average throughput and outage capacity expressions are derived for RIS-aided communication systems considering multiple RISs. Stochastic ordering results for the normalized k -th maximum SNR RV are also presented.

The organization of the paper is as follows. Section II introduces the considered system model for RIS-aided communication systems. Section III presents the results of k -th maximum order statistics of NCCS RVs with one d.o.f and derives the average throughput and outage capacity expressions for RIS-aided communication systems in a multi-RIS scenario. Section IV provides extensive simulation results to support our theoretical analysis, and Section V concludes the paper.

The following notations are used in the paper. The probability density function and cumulative distribution functions of an RV X are denoted by $f_X(\cdot)$ and $F_X(\cdot)$, respectively. The expectation of RV X is denoted as $\mathbb{E}(X)$. Given an event A , $\mathbb{P}(A)$ denotes the probability of the event A .

II. SYSTEM MODEL

In this work, we consider a RIS-aided wireless communication system model as shown in Fig. 1. It has a source (S), destination (D), and R number of RISs. The source and destination have a single antenna, and the r^{th} RIS has N_r reflecting elements. Different RISs can have different numbers of reflecting elements. Similar to [34], we assume that there is no direct link between the source and destination due to the outage. Here, RISs act as passive reflectors between the source and destination and improve the quality of the signal at the receiver. Each RIS will reflect the signal transmitted by the source to the destination, so there are R links available at the receiver

for processing. Similar to [22], [34], [48], [49], we assume that each RIS is controlled to steer their beam to the destination, avoiding interference with each other. The link with the highest quality is selected for communication between the source and destination in an opportunistic multi-RIS environment [34].

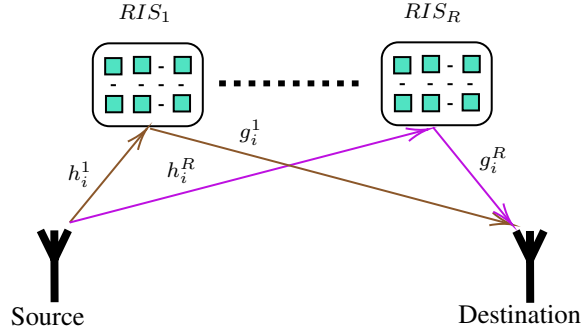


Fig. 1: System Model

Let h_i^r and g_i^r represent the channel fading coefficients between the source to i^{th} reflecting element of r^{th} RIS, and i^{th} reflecting element of r^{th} RIS to destination respectively. Also, all the channels are assumed to undergo independent Rayleigh fading. Let x be the transmitted signal, then the received signal at the destination reflected from r^{th} RIS is given by

$$y^r = \sqrt{P_s} \left[\sum_{i=1}^{N_r} h_i^r \exp(j\phi_i^r) g_i^r \right] x + n^r, \quad (1)$$

where P_s is the source transmit power and n^r is the additive white Gaussian noise (AWGN) with mean zero and variance V_0 . Assume d_{sr} and d_{rd} are the distances between source to r^{th} RIS and r^{th} RIS to destination, respectively. The small-scale fading channel gains are given by $h_i^r = \eta_i^r e^{-j\theta_i^r}$ and $g_i^r = \beta_i^r e^{-j\psi_i^r}$. Here η_i^r , θ_i^r represent the channel amplitude and phase, respectively, for the link between source and r^{th} RIS. Similarly, β_i^r , ψ_i^r represent the channel amplitude and phase, respectively, for the link between r^{th} RIS and destination. Similar to [20] and using (1), instantaneous SNR at destination from r^{th} RIS is given by

$$\gamma^r = \frac{P_s \left| \sum_{i=1}^{N_r} \eta_i^r \beta_i^r e^{j(\phi_i^r - \theta_i^r - \psi_i^r)} \right|^2}{V_0}. \quad (2)$$

Similar to [20], full channel state information is assumed to be available. So γ^r can be maximized by setting the $\phi_i^r = \theta_i^r + \psi_i^r$. Therefore γ^r can be written as

$$\gamma^r = \frac{P_s \left(\sum_{i=1}^{N_r} \eta_i^r \beta_i^r \right)^2}{V_0} = \bar{\gamma} A_r^2, \quad (3)$$

where $A^r = \sum_{i=1}^{N_r} \eta_i^r \beta_i^r$ and average SNR $\bar{\gamma} = \frac{P_s}{V_0}$.

At the destination, the RIS with the highest SNR is selected for communication. Assuming $\bar{\gamma}$ is the average channel SNR in the past window [34], the selection principle at the destination similar to [34] is given by

$$\hat{r} = \arg \max_{r=1, \dots, R} \gamma^r, \quad (4)$$

where $\gamma^r = A_r^2$. As the number of reflecting surfaces in RIS becomes large $N_r \gg 1$, using central limit theorem (CLT) it is shown [20], [21] that A_r follows Gaussian distribution with mean $\frac{N_r \pi}{4}$ and variance of $N_r \left(1 - \frac{\pi^2}{16}\right)$. Hence, we can see that A_r^2 will be an NCCS RV with one d.o.f.

Considering a source, destination, and R RISs in between, R links with SNRs $\{\gamma^r\}_{r=1}^R$ are available at the destination. Each γ^r follows a NCCS distribution with one d.o.f with the parameters $\lambda_r = \left(\frac{N_r \pi}{4}\right)^2$ and $\sigma_r^2 = N_r \left(1 - \frac{\pi^2}{16}\right)$. Here, λ_r represents the non-centrality parameter, and σ_r^2 is the variance of NCCS distribution. Typically, the link with the highest SNR is selected for communication.

$$\gamma_{max}^R = \gamma_{\hat{r}} = \max_{r=1, \dots, R} \gamma^r. \quad (5)$$

Now let us see how we find the distribution of maximum SNR (γ_{max}^R). Observe that parameters (λ_r, σ_r) of NCCS RVs depend on the number of reflecting elements (N_r) of r^{th} RIS. So, if we consider an equal number of reflecting elements on each RIS, then γ_{max}^R would be the maximum of R i.i.d NCCS RVs with one d.o.f. This was the case studied in [34]. Different numbers of reflecting elements will result in γ_{max}^R being the maximum of i.n.i.d. NCCS RVs. The exact distribution of γ_{max}^R can be written as $F_{\gamma_{max}^R}(\gamma) = \prod_{r=1}^R F_{\gamma^r}(\gamma)$ and the exact distribution of γ_{max}^R will involve fairly complicated expressions whose complexity increasing with increasing R . Instead, we will utilize the EVT to characterize the asymptotic distribution of maximum order statistics of i.n.i.d. NCCS RVs with one d.o.f in the next section.

III. MAXIMUM ORDER STATISTICS OF I.N.I.D. NCCS RVs

The general procedure in finding the asymptotic distribution of maximum order statistics for i.i.d. RVs involves finding the maximum domain of attraction of the common distribution function. However, in the case of i.n.i.d. RVs, additional requirements have to be met in order for the maxima to be a non-degenerate distribution. Finding appropriate normalizing constants which satisfies the additional requirements is fairly challenging. In this section, we derive

the maximum order statistics of a sequence of i.n.i.d. NCCS RVs with one d.o.f using EVT. Considering the normalizing constants a_R and b_R , first, we will derive the asymptotic distribution of the normalized maximum SNR ($\tilde{\gamma}_{max}$) where $\tilde{\gamma}_{max} = \lim_{R \rightarrow \infty} \frac{\gamma_{max}^R - b_R}{a_R}$. Once we have $\tilde{\gamma}_{max}$, characterization of γ_{max}^R is simple. We will introduce some of EVT's key results from [45] for the general i.n.i.d. case in order to facilitate the understanding of our proofs.

Let $\{\gamma_1, \gamma_2, \dots, \gamma_R\}$ be a sequence of independent random variables with $\gamma_r \sim F_r(\gamma)$ for $r = 1, 2, \dots, R$. If $\gamma_{max}^R = \max\{\gamma_r\}_{r=1}^R$, then CDF of γ_{max}^R can be written as

$$G_{max}^R(\gamma) = P(\gamma_{max}^R \leq \gamma) = \prod_{r=1}^R F_r(\gamma). \quad (6)$$

The following uniformity assumptions (UAs) are required for the analysis of asymptotic order statistics. The sequences of CDFs $F_r(\gamma)$ and normalizing constants a_R and b_R are said to satisfy the UAs for maximum vector γ_{max}^R if

$$\max_{1 \leq r \leq R} \{1 - F_r(a_R \gamma + b_R)\} \rightarrow 0 \quad \text{as } R \rightarrow \infty, \quad (7)$$

for all $a_R \gamma + b_R > \alpha(F_r)$ and $\alpha(F_r) := \inf\{\gamma : F_r(\gamma) > 0\} > -\infty$. Also, for a fixed number $0 < t \leq 1$ and each sequence of integers $\{m_R\}_R$ such that $m_R < R$, when $R \rightarrow \infty$, $m_R \rightarrow \infty$ and $\frac{m_R}{R} \rightarrow t$, we should have that

$$\tilde{u}(t, \gamma) = \lim_{R \rightarrow \infty} \sum_{r=1}^{m_R} (1 - F_r(a_R \gamma + b_R)), \quad (8)$$

exists and is finite for all $0 < t \leq 1$, whenever it is finite for $t = 1$. With the UAs in (7) and (8), the authors of [45] presented the following lemma for characterizing the asymptotic distribution of the maximum random variable for the general i.n.i.d. case.

Lemma 1. *Under the UA (7) and (8), a non-degenerate CDF $\tilde{G}_{max}(\gamma)$ is the asymptotic distribution of $\frac{\gamma_{max}^R - b_R}{a_R}$ i.e., $G_{max}^R(a_R \gamma + b_R) = \prod_{r=1}^R F_r(a_R \gamma + b_R) \xrightarrow{D} \tilde{G}_{max}(\gamma)$ as $R \rightarrow \infty$ where \xrightarrow{D} stands for convergence in distribution, if and only if*

$$\tilde{u}(\gamma) = \tilde{u}(1, \gamma) = \lim_{R \rightarrow \infty} \sum_{r=1}^R (1 - F_r(a_R \gamma + b_R)) < \infty. \quad (9)$$

Moreover $\tilde{G}_{max}(\gamma)$ should have the form $\tilde{G}_{max}(\gamma) = e^{-\tilde{u}(\gamma)}$ and either (i) $\log \tilde{G}_{max}(\gamma)$ is concave or (ii) $\omega_{max} = \omega(\tilde{G}_{max}(\gamma))$ is finite and $\log \tilde{G}_{max}(\omega_{max} - e^{-\gamma})$ is concave or (iii) $\alpha_{max} = \alpha(\tilde{G}_{max}(\gamma))$ is finite and $\log \tilde{G}_{max}(\alpha_{max} - e^{-\gamma})$ is concave where $\gamma > 0$ in (ii) and (iii).

Proof. Please refer to [45] for the proof. \square

We will make use of Lemma 1 in deriving the asymptotic distribution of the random variable $\tilde{\gamma}_{max}$ by arriving at normalizing constants a_R and b_R , satisfying the UAs and (9) for i.n.i.d. NCCS RVs. Once we arrive at $\tilde{\gamma}_{max}$, using this, we can obtain the distribution of γ_{max}^R .

Now, we will consider the system model presented in Section II to derive the asymptotic distribution of γ_{max}^R . Note that considering different numbers of reflecting elements in each RIS, we must deal with i.n.i.d. RVs $\{\gamma^r\}_{r=1}^R$. And, if we assume the same number of reflecting elements for all the RISs, we will get i.i.d. RVs $\{\gamma^r = \gamma\}_{r=1}^R$.

A. i.n.i.d. case

Now, let $\{\gamma^r\}_{r=1}^R$ be a sequence of NCCS random variables with one d.o.f, then its CDF is

$$F_{\gamma^r}(\gamma) = 1 - Q_{\frac{1}{2}}\left(\frac{\sqrt{\lambda_r}}{\sigma_r}, \frac{\sqrt{\gamma}}{\sigma_r}\right). \quad (10)$$

In (10), $Q_{\frac{1}{2}}(\cdot, \cdot)$ is the Marcum-Q function [50] and λ_r is the non-centrality parameter of the non-central chi-square RV. As mentioned in section II, $\lambda_r = \left(\frac{N_r\pi}{4}\right)^2$ and $\sigma_r^2 = N_r \left(1 - \frac{\pi^2}{16}\right)$ depends only on the number of reflecting elements and both λ_r and σ_r will take maximum value at same index corresponding to RIS with maximum number of reflecting elements. Let R be the total number of RVs. We will assume (λ_r, σ_r) takes a finite set of values i.e. $\lambda_r \in \{\lambda_1, \lambda_2 \dots \lambda_P\}$ for all $r \in \{1, \dots R\}$ and $\sigma_r \in \{\sigma_1, \sigma_2 \dots \sigma_P\}$ for all $r \in \{1, \dots R\}$. Define

$$R_i = \sum_{r=1}^R \mathbb{I}_{\lambda_r = \lambda_i, \sigma_r = \sigma_i} \quad 1 \leq i \leq P,$$

Where $\mathbb{I}_{\lambda_r, \sigma_r} := \begin{cases} 1 & \text{if } \lambda_r = \lambda_i, \sigma_r = \sigma_i \\ 0 & \text{if } \lambda_r \neq \lambda_i, \sigma_r \neq \sigma_i \end{cases}$. Here R_i represents the number of times pair (λ_i, σ_i)

occurs among R values. In the case of the multi-RIS system model presented in section II, the SNR follows the CDF in (10).

Theorem 1. *The asymptotic CDF of normalized maximum ($\tilde{\gamma}_{max}$) of a sequence of i.n.i.d. non-central chi-square random variables with one d.o.f as $R \rightarrow \infty$ is given by*

$$F_{\tilde{\gamma}_{max}}(\gamma) = \exp(-\exp(-\gamma)), \quad (11)$$

for normalizing constants $a_R = \frac{\tilde{\sigma}^2}{\epsilon}$ and $b_R = \frac{\tilde{\sigma}^2}{\epsilon} \left[\log(\tilde{R}) - c_1\right]$. Here, (λ_r, σ_r) takes a finite set of values i.e. $\lambda_r \in \{\lambda_1, \lambda_2 \dots \lambda_P\}$ and $\sigma_r \in \{\sigma_1, \sigma_2 \dots \sigma_P\}$ for all $r \in \{1, \dots R\}$. Further,

R_i represents the number of times pair (λ_i, σ_i) occurs among R values. Let $\tilde{\sigma}$ be the largest among $\{\sigma_1, \dots, \sigma_P\}$, $\tilde{\lambda}$ be the largest among $\{\lambda_1, \dots, \lambda_P\}$ and \tilde{R} to be the largest among $\{R_1, \dots, R_P\}$. Also, ϵ is the Chernoff parameter ($0 < \epsilon < \frac{1}{2}$) and

$$c_1 = \frac{-1}{\tilde{\theta}} \left[\log(1 - 2\epsilon)^{-\frac{1}{2}} + \frac{\epsilon}{2(1 - 2\epsilon)} \frac{\tilde{\lambda}}{\tilde{\sigma}^2} \right].$$

Proof. Lemma 1 states that if

$$\tilde{u}(\gamma) = \lim_{R \rightarrow \infty} \sum_{r=1}^R (1 - F_r(a_R \gamma + b_R)) < \infty, \quad (12)$$

for some normalizing constants a_R and b_R satisfying UAs, we can derive the distribution of $\tilde{\gamma}_{max}$. Further, Mezlers [51, Chapter 5] give the following conditions on a_R and b_R such that UA (7) and (8) are satisfied:

$$|\log a_R| + |b_R| \rightarrow \infty \text{ as } R \rightarrow \infty, \quad (13)$$

and

$$\begin{aligned} \frac{a_{R+1}}{a_R} &\rightarrow 1, \\ \frac{(b_{R+1} - b_R)}{a_R} &\rightarrow 0. \end{aligned} \quad (14)$$

We will derive the distribution of $\tilde{\gamma}_{max}$ by finding a a_R and a b_R such that (12), (13) and (14) are satisfied in order for the UAs to hold. From [34, (18)], the asymptotic form of the generalized Marcum Q-function can be expressed as

$$Q_n(x, y) \simeq (1 - 2\epsilon)^{-n} \exp(-\epsilon y^2) \exp\left(\frac{n\epsilon x^2}{1 - 2\epsilon}\right). \quad (15)$$

Here $y^2 > n(x^2 + 2)$ and ϵ is the Chernoff parameter ($0 < \epsilon < \frac{1}{2}$) with optimum value $\epsilon_0 = \frac{1}{2} \left(1 - \frac{n}{y^2} - \frac{n}{y^2} \sqrt{1 + \frac{x^2 y^2}{n}}\right)$ Using (15) and (10), we can rewrite $\tilde{u}(\gamma)$ in (12) as

$$\tilde{u}(\gamma) = \lim_{R \rightarrow \infty} \sum_{i=1}^R R_i (1 - 2\epsilon)^{-\frac{1}{2}} \exp\left(-\frac{\epsilon}{\sigma_i^2} (a_R \gamma + b_R)\right) \exp\left(\frac{\epsilon}{2(1 - 2\epsilon)} \frac{\lambda_i}{\sigma_i^2}\right) \quad (16)$$

$$\tilde{u}(\gamma) = \lim_{R \rightarrow \infty} \sum_{i=1}^R R_i (1 - 2\epsilon)^{-\frac{1}{2}} \exp\left(\frac{\epsilon}{2(1 - 2\epsilon)} \frac{\lambda_i}{\sigma_i^2}\right) \exp\left(-\frac{\epsilon}{\sigma_i^2} (a_R \gamma)\right) \exp\left(-\frac{\epsilon}{\sigma_i^2} (b_R)\right) \quad (17)$$

Choose $\tilde{\sigma}$ to be the largest among $\{\sigma_1, \dots, \sigma_P\}$, $\tilde{\lambda}$ to be the largest among $\{\lambda_1, \dots, \lambda_P\}$ and \tilde{R} to be the largest among $\{R_1, \dots, R_P\}$. Let us assume the following a_R and b_R values satisfying the conditions in (13) and (14)

$$a_R = \frac{\tilde{\sigma}^2}{\epsilon}, \quad (18)$$

and

$$b_R = \frac{\tilde{\sigma}^2}{\epsilon} \left[\log(\tilde{R}) - c_1 \right], \quad (19)$$

where c_1 is a constant and we assume $\tilde{R} \rightarrow \infty$ as $R \rightarrow \infty$. Note a_R and b_R satisfy (13) and (14). For the above choice of normalizing constant, UA (7) is satisfied as $b_R \rightarrow \infty$ as $R \rightarrow \infty$. For UA (8) to be satisfied, we require $\tilde{u}(\gamma) < \infty$ and a_R and b_R should satisfy (13) and (14). Substituting a_R and b_R in (17),

$$\begin{aligned} \tilde{u}(\gamma) = \lim_{R \rightarrow \infty} \sum_{i=1}^R R_i (1-2\epsilon)^{-\frac{1}{2}} \exp \left(\frac{\epsilon}{2(1-2\epsilon)} \frac{\lambda_i}{\sigma_i^2} \right) \\ \exp \left(-\frac{\epsilon}{\sigma_i^2} \left(\frac{\tilde{\sigma}^2}{\epsilon} \gamma \right) \right) \exp \left(-\frac{\epsilon}{\sigma_i^2} \left(\frac{\tilde{\sigma}^2}{\epsilon} \left[\log(\tilde{R}) - c_1 \right] \right) \right). \end{aligned} \quad (20)$$

Let $\left(\frac{\tilde{\sigma}}{\sigma_i} \right)^2 = \theta_i$, so $\theta_i \in \{\theta_1, \theta_2 \dots \theta_P\}$.

$$\tilde{u}(\gamma) = \lim_{R \rightarrow \infty} \sum_{i=1}^R R_i (1-2\epsilon)^{-\frac{1}{2}} \exp \left(\frac{\epsilon}{2(1-2\epsilon)} \frac{\lambda_i}{\sigma_i^2} \right) \exp(-\theta_i \gamma) \exp(-\theta_i \log(\tilde{R}) + \theta_i c_1). \quad (21)$$

After rearranging (21), we have,

$$\tilde{u}(\gamma) = \lim_{R \rightarrow \infty} \sum_{i=1}^R \exp(-\theta_i \gamma) \underbrace{\frac{R_i}{\tilde{R}^{\theta_i}} (1-2\epsilon)^{-\frac{1}{2}} \exp \left(\frac{\epsilon}{2(1-2\epsilon)} \frac{\lambda_i}{\sigma_i^2} \right) \exp(\theta_i c_1)}_{\text{Term-1}} \quad (22)$$

$$\tilde{u}(\gamma) = \lim_{R \rightarrow \infty} \sum_{i=1}^R \exp(-\theta_i \gamma) \underbrace{\frac{R_i}{\tilde{R}^{\theta_i}} \exp \left(\log((1-2\epsilon)^{-\frac{1}{2}} + \frac{\epsilon}{2(1-2\epsilon)} \frac{\lambda_i}{\sigma_i^2} + \theta_i c_1) \right)}_{\text{Term-1}} \quad (23)$$

Let us find the constant c_1 from Term-1, i.e. obtain c_1 such that

$$\theta_i c_1 = -\log(1-2\epsilon)^{-\frac{1}{2}} - \frac{\epsilon}{2(1-2\epsilon)} \frac{\lambda_i}{\sigma_i^2}.$$

Choose $c_1 = \frac{-1}{\tilde{\theta}} \left[\log(1-2\epsilon)^{-\frac{1}{2}} + \frac{\epsilon}{2(1-2\epsilon)} \frac{\tilde{\lambda}}{\tilde{\sigma}^2} \right]$, where $\tilde{\theta} = \min_{i=1,2,\dots,P} \theta_i$ so that Term-1 in (23) will become one for $\tilde{\sigma} = \sigma_i$. Note that θ_i takes values greater than or equal to one, and when $\tilde{\sigma} = \sigma_i$ then only $\theta_i = 1$. Substituting c_1 in (23)

$$\begin{aligned} \tilde{u}(\gamma) = \lim_{R \rightarrow \infty} \sum_{i=1}^R \exp(-\theta_i \gamma) \frac{R_i}{\tilde{R}^{\theta_i}} \exp \left(\log(1-2\epsilon)^{-\frac{1}{2}} + \frac{\epsilon}{2(1-2\epsilon)} \frac{\lambda_i}{\sigma_i^2} \right) \\ \exp \left(-\frac{\theta_i}{\tilde{\theta}} \left[\log(1-2\epsilon)^{-\frac{1}{2}} + \frac{\epsilon}{2(1-2\epsilon)} \frac{\tilde{\lambda}}{\tilde{\sigma}^2} \right] \right). \end{aligned} \quad (24)$$

Therefore,

$$\tilde{u}(\gamma) = \sum_{i=1}^P (\exp(-\theta_i \gamma) p_i), \quad (25)$$

where $p_i = \frac{R_i}{\tilde{R}^{\theta_i}} \exp\left(\log(1-2\epsilon)^{-\frac{1}{2}} + \frac{\epsilon}{2(1-2\epsilon)} \frac{\lambda_i}{\sigma_i^2}\right) \exp\left(-\frac{\theta_i}{\theta} \left[\log(1-2\epsilon)^{-\frac{1}{2}} + \frac{\epsilon}{2(1-2\epsilon)} \frac{\tilde{\lambda}}{\tilde{\sigma}^2}\right]\right)$. Note that $\tilde{R} \rightarrow \infty$ when $R \rightarrow \infty$ and there are P values for p_i i.e., $i = 1, 2, \dots, P$. Only for one i ($\lambda_i = \tilde{\lambda}, \sigma_i = \tilde{\sigma}$), $\theta_i = 1$ and in that scenario $p_i = 1$ because $R_i = \tilde{R}$ and all the terms in the exponent go to zero. Also, for this case $\tilde{u}(\gamma)$ is finite as $\lim_{R \rightarrow \infty} \frac{R_i}{\tilde{R}^{\theta_i}} = 1$. For all remaining i 's ($\lambda_i \neq \tilde{\lambda}, \sigma_i \neq \tilde{\sigma}$) as $R_i < \tilde{R}$ and $\theta_i > 1$ corresponding $p_i = 0$ as $\lim_{R \rightarrow \infty} \frac{R_i}{\tilde{R}^{\theta_i}} = 0$. Hence, the summation in (25) is finite making $\tilde{u}(\gamma) = \exp(-\gamma) < \infty$ for the choice of normalizing constants $a_R = \frac{\tilde{\sigma}^2}{\epsilon}$ and $b_R = \frac{\tilde{\sigma}^2}{\epsilon} [\log(\tilde{R}) - c_1]$. Furthermore, from Lemma 1 $\tilde{G}_{max}(\gamma) = e^{-\tilde{u}(\gamma)} = \exp(-\exp(-\gamma))$ and note that $\log \tilde{G}_{max}(\gamma) = -\exp(-\gamma)$ is concave. Hence, the asymptotic CDF of the normalized maximum of a non-central chi-square RVs with one d.o.f is given by

$$F_{\tilde{\gamma}_{max}}(\gamma) = \exp(-\exp(-\gamma)). \quad (26)$$

Note that for all practical purposes (finite values of R and \tilde{R}), one can still use $\tilde{u}(\gamma) = \sum_{i=1}^P (\exp(-\theta_i \gamma) p_i)$ and

$$F_{\tilde{\gamma}_{max}}(\gamma) = \exp\left(-\sum_{i=1}^P (\exp(-\theta_i \gamma) p_i)\right), \quad (27)$$

where $p_i = \frac{R_i}{\tilde{R}^{\theta_i}} \exp\left(\log(1-2\epsilon)^{-\frac{1}{2}} + \frac{\epsilon}{2(1-2\epsilon)} \frac{\lambda_i}{\sigma_i^2}\right) \exp\left(-\frac{\theta_i}{\theta} \left[\log(1-2\epsilon)^{-\frac{1}{2}} + \frac{\epsilon}{2(1-2\epsilon)} \frac{\tilde{\lambda}}{\tilde{\sigma}^2}\right]\right)$. \square

B. i.i.d. case

If all the RISs have the same number of reflecting elements ($N_r = N$), then each γ^r follows an NCCS distribution with one d.o.f with the parameters $\lambda_r = \left(\frac{N\pi}{4}\right)^2$ and $\sigma_r^2 = N \left(1 - \frac{\pi^2}{16}\right)$. So $\gamma_{max} = \max_{r=1,2,\dots,P} \{\gamma^r = \gamma\}$ and distribution of normalized maximum $F_{\tilde{\gamma}_{max}}(\gamma)$ can be derived as a special case of Theorem 1 and is presented in the following corollary.

Corollary 1.1. *The asymptotic CDF of $\tilde{\gamma}_{max}$ of a sequence of i.i.d. non-central chi-square random variables with one d.o.f as $R \rightarrow \infty$ is given by*

$$F_{\tilde{\gamma}_{max}}(\gamma) = \exp[-\exp(-\gamma)], \quad (28)$$

for normalizing constants $a_R = \frac{\sigma^2}{\epsilon}$ and $b_R = \frac{\sigma^2}{\epsilon} [\log(R) - c_1]$. Also, ϵ is the Chernoff parameter ($0 < \epsilon < \frac{1}{2}$) and $c_1 = -\left[\log(1-2\epsilon)^{-\frac{1}{2}} + \frac{\epsilon}{2(1-2\epsilon)} \frac{\lambda}{\sigma^2}\right]$ are constants.

Proof. This result can be derived by substituting $\lambda_r = \lambda$ and $\sigma_r = \sigma$ for all $r = \{1, 2, \dots, P\}$ in Theorem 1. \square

For all practical cases one can obtain the unnormalized statistics by substituting γ by $\frac{\gamma - b_R}{a_R}$ in (26). Therefore $F_{\gamma_{max}}(\gamma)$ can be written as

$$F_{\gamma_{max}}(\gamma) = F_{\tilde{\gamma}_{max}}(\gamma) \Big|_{\gamma = \frac{\gamma - b_R}{a_R}}. \quad (29)$$

C. k -th order statistics

So far, we have analyzed the multi-RIS system in a scenario where the link with the highest SNR is selected. If we are interested in choosing the link with k -th highest SNR instead of maximum SNR, we require the k -th order statistics, i.e., we want to find the normalized k -th maximum distribution of NCCS random variables with one d.o.f. Let $\gamma_{(1:R)} \leq \gamma_{(2:R)} \leq \dots \leq \gamma_{(R:R)}$, be the order statistics where the k -th order statistic is given by $\gamma_{(R-k+1:R)}$. Finding the exact CDF of k -th order statistic $\gamma_{(R-k+1:R)}$ involves very complicated expression as given [52, (5.2.1)]

$$F_{\gamma_{(R-k+1:R)}}(\gamma) = \sum_{m=k}^R \sum_{S_m} \prod_{r=1}^m F_{\gamma_{j_r}}(\gamma) \times \prod_{r=m+1}^R [1 - F_{\gamma_{j_r}}(\gamma)], \quad k = 1, 2, \dots, R, \quad (30)$$

where the summation S_m is over all the permutations (j_1, \dots, j_R) of $1, \dots, R$ for which $j_1 < \dots < j_m$ and $j_{m+1} < \dots < j_R$. A simpler asymptotic CDF of $\gamma_{(R-k+1:R)}$ can be computed with the help of EVT. Asymptotic order statistics can be derived with the help of the results presented in [53]. For ease of understanding, we will repeat an important Lemma here

Lemma 2. Assume that for suitable normalizing constants $a_R > 0$, b_R

$$\delta_R = \max_{1 \leq r \leq R} 1 - F_{\gamma_r}(a_R \gamma + b_R) \rightarrow 0 \text{ as } R \rightarrow \infty. \quad (31)$$

Then $\tilde{\phi}_{k:R}(\gamma) = \mathbb{P}\left(\frac{\gamma_{(R-k+1:R)} - b_R}{a_R} \leq \gamma\right)$ converges weakly to a non degenerate distribution function $\tilde{\phi}_k(\gamma)$ if and only if, for all γ for which $\tilde{\phi}_k(\gamma) > 0$, the limit

$$\tilde{u}(\gamma) = \lim_{R \rightarrow \infty} \sum_{r=1}^R 1 - F_{\gamma_r}(a_R \gamma + b_R) \text{ is finite,} \quad (32)$$

and the function

$$\tilde{\phi}_k(\gamma) = \sum_{r=0}^{k-1} \frac{\tilde{u}^r(\gamma)}{r!} \exp(-\tilde{u}(\gamma)), \text{ is a non degenerate distribution.} \quad (33)$$

The actual limit of $\tilde{\gamma}_{(R-k+1:R)} = \frac{\gamma_{(R-k+1:R)} - b_R}{a_R}$ is the one given in (33).

Proof. Please refer [53] for the detailed proof. \square

Now, we use Lemma 2 to derive the k -th order statistics of i.n.i.d. NCCS random variables with one d.o.f for the system model presented in section II. We can observe that in (25), we have already proved that $\tilde{u}(\gamma)$ is finite for the normalizing constants $a_R = \frac{\tilde{\sigma}^2}{\epsilon}$ and $b_R = \frac{\tilde{\sigma}^2}{\epsilon} \left[\log(\tilde{R}) - c_1 \right]$ satisfying the UA (7) and (8). For k -th order statistics also, we need to satisfy the equations (31) and (32), which are same as UA (7) and (8). Hence, we can utilize the obtained $\tilde{u}(\gamma)$ from (26). So, if we substitute the derived $\tilde{u}(\gamma)$ in (33) and show that $\tilde{\phi}_k$ is a non-degenerate distribution, then we obtain the normalized distribution of k -th order statistics. We present the results in the following corollary.

Corollary 1.2. *The asymptotic CDF of normalized k -th maximum of a sequence of i.n.i.d. non-central chi-square random variables with one d.o.f as $R \rightarrow \infty$ is given by,*

$$\tilde{\phi}_k(\gamma) = \sum_{r=0}^{k-1} \frac{(\tilde{u}(\gamma))^r}{r!} \exp(-\tilde{u}(\gamma)) = F_{\tilde{\gamma}_{(R-k+1:R)}}(\gamma) = \frac{\Gamma(k, \tilde{u}(\gamma))}{\Gamma(k)}, \quad (34)$$

where

$$\tilde{u}(\gamma) = \exp(-\gamma), \quad (35)$$

for normalizing constants $a_R = \frac{\tilde{\sigma}^2}{\epsilon}$ and $b_R = \frac{\tilde{\sigma}^2}{\epsilon} \left[\log(\tilde{R}) - c_1 \right]$. Assume (λ_r, σ_r) takes a finite set of values i.e. $\lambda_r \in \{\lambda_1, \lambda_2 \dots \lambda_P\}$ and $\sigma_r \in \{\sigma_1, \sigma_2 \dots \sigma_P\}$ for all $r \in \{1, \dots, R\}$. Further, R_i represents the number of times pair (λ_i, σ_i) occurs among R values. Let $\tilde{\sigma}$ be the largest among $\{\sigma_1, \dots, \sigma_P\}$ and $\tilde{\lambda}$ be the largest among $\{\lambda_1, \dots, \lambda_P\}$ and also \tilde{R} be the largest among $\{R_1, \dots, R_P\}$. Also, ϵ is the Chernoff parameter ($0 < \epsilon < \frac{1}{2}$) and $c_1 = \frac{-1}{\theta} \left[\log(1 - 2\epsilon)^{-\frac{1}{2}} + \frac{\epsilon}{2(1-2\epsilon)} \frac{\tilde{\lambda}}{\tilde{\sigma}^2} \right]$.

Proof. The results can be derived by substituting $\tilde{u}(\gamma)$ derived in (26) into (33)

$$\tilde{\phi}_k(\gamma) = \sum_{r=0}^{k-1} \frac{(\exp(-\gamma))^r}{r!} \exp(-\exp(-\gamma)). \quad (36)$$

The upper incomplete gamma function for integer k [54] can be written as

$$\Gamma(k, x) = (k-1)! e^{-x} \sum_{r=0}^{k-1} \frac{x^r}{r!}.$$

Using the $\Gamma(k, x)$ and $\Gamma(x) = (x - 1)!$ for integer x [55], we can rewrite (36) as

$$\tilde{\phi}_k(\gamma) = F_{\tilde{\gamma}_{(R-k+1:R)}}(\gamma) = \frac{\Gamma(k, \tilde{u}(\gamma))}{\Gamma(k)}. \quad (37)$$

Note that now, $\tilde{\phi}_k(\gamma)$ is a non degenerate function as $\frac{\Gamma(k, \tilde{u}(\gamma))}{\Gamma(k)}$ is not a one point distribution. \square

Here also, we can note that for all practical purposes, one can use $\tilde{u}(\gamma) = \sum_{i=1}^P (\exp(-\theta_i \gamma) p_i)$ with $p_i = \frac{R_i}{R^{\theta_i}} \exp\left(\log(1 - 2\epsilon)^{-\frac{1}{2}} + \frac{\epsilon}{2(1-2\epsilon)} \frac{\lambda_i}{\sigma_i^2}\right) \exp\left(-\frac{\theta_i}{\theta} \left[\log(1 - 2\epsilon)^{-\frac{1}{2}} + \frac{\epsilon}{2(1-2\epsilon)} \frac{\tilde{\lambda}}{\tilde{\sigma}^2}\right]\right)$. We can observe that once we have the results for normalized k -th order statistics, we can derive the results for unnormalized k -th order statistics by substituting γ by $\frac{\gamma - b_R}{a_R}$ in (34).

D. Stochastic ordering of k -th maximum SNR

The CDF of k -th maximum RV in terms of normalizing constants can be written as

$$F_{\tilde{\gamma}_{(R-k+1:R)}}(\gamma) = \frac{\Gamma\left(k, \tilde{u}\left(\frac{\gamma - b_R}{a_R}\right)\right)}{\Gamma(k)}.$$

Let A and B are two k -th maximum RVs with normalizing constants (a_R^A, b_R^A) and (a_R^B, b_R^B) respectively. From stochastic ordering, an RV A is stochastically smaller than RV B if [47]

$$\mathbb{P}(A > z) \leq \mathbb{P}(B > z) \quad \forall z \in \mathbb{R}. \quad (38)$$

We can write the same in terms of CDF expressions in the following form

$$\Gamma\left(k, \tilde{u}\left(\frac{\gamma - b_R^B}{a_R^B}\right)\right) \leq \Gamma\left(k, \tilde{u}\left(\frac{\gamma - b_R^A}{a_R^A}\right)\right). \quad (39)$$

As $\Gamma(k, x)$ is a decreasing function with respect to its argument x , the inequality (39) is true if $\tilde{u}\left(\frac{\gamma - b_R^B}{a_R^B}\right) \geq \tilde{u}\left(\frac{\gamma - b_R^A}{a_R^A}\right)$, i.e.

$$\exp\left(\frac{-\gamma + b_R^B}{a_R^B}\right) \geq \exp\left(\frac{-\gamma + b_R^A}{a_R^A}\right).$$

We can observe that closed-form expressions of normalizing constants have a one-to-one mapping with the parameters, as shown below

$$a_R^I = \frac{\tilde{\sigma}_I^2}{\epsilon},$$

$$b_R^I = \frac{\tilde{\sigma}_I^2}{\epsilon} \left[\log(\tilde{R}_I) + \frac{1}{\theta_I} \left(\log(1 - 2\epsilon)^{-\frac{1}{2}} + \frac{\epsilon}{2(1-2\epsilon)} \frac{\tilde{\lambda}_I}{\tilde{\sigma}_I^2} \right) \right],$$

where $I \in \{A, B\}$. Here, any parameter changes are reflected in corresponding normalizing constants. Hence, stochastic ordering can be established as the expressions for normalizing constants have the corresponding mapping with the parameters.

E. Average Throughput and Outage Capacity

In this subsection, we will derive the expression for multiple RIS-aided communication systems' average throughput and outage capacity. Here, we consider the received SNR at the destination as the k -th maximum order statistics following the CDF expression presented in (34). Also, here we will consider the SNR random variable to be of type $\gamma_a \gamma_{(R-k+1:R)}$ where γ_a is a constant.

1) *Average Throughput* : Given the CDF of normalized k -th maximum ($\gamma_{(R-k+1:R)}$) of i.n.i.d. NCCS RVs with one d.o.f (34), we can derive the average throughput at the receiver. The expression for average throughput can be written as

$$C_{R-k+1:R} = \mathbb{E} \left[\log_2 (1 + \gamma_a \gamma_{(R-k+1:R)}) \right]. \quad (40)$$

The expression in (40) can be solved using the following numerical integration.

$$C_{R-k+1:R} = \int_0^\infty \log_2 (1 + \gamma_a \gamma_{(R-k+1:R)}) f_{\gamma_{(R-k+1:R)}}(\gamma) d\gamma. \quad (41)$$

Here, $f_{\gamma_{(R-k+1:R)}}(\gamma)$ is the pdf of k -th maximum i.e. $\gamma_{(R-k+1:R)}$. The pdf expression of $f_{\gamma_{(R-k+1:R)}}(\gamma)$ can be obtained by differentiating the CDF expression in (34) and can be written as

$$f_{\gamma_{(R-k+1:R)}}(\gamma) = \frac{1}{a_R \Gamma(k)} \exp \left(- \exp \left(- \frac{\gamma - b_R}{a_R} \right) \right) \left(\exp \left(- \frac{\gamma - b_R}{a_R} \right) \right)^k. \quad (42)$$

Hence average throughput can be calculated by substituting $f_{\gamma_{(R-k+1:R)}}(\gamma)$ in (41) with the help of numerical integration routines.

2) *Outage Capacity*: Given the CDF of k -th maximum (34), the outage probability for a threshold γ_{th} can be calculated as

$$P_{out} = \mathbb{P} (\gamma_a \gamma_{(R-k+1:R)} \leq \gamma_{th}) = F_{\gamma_{(R-k+1:R)}} \left(\frac{\gamma_{th}}{\gamma_a} \right) = \frac{\Gamma \left(k, \tilde{u} \left(\frac{\gamma_{th} - b_R}{a_R} \right) \right)}{\Gamma(k)}. \quad (43)$$

Similarly, Outage capacity can be calculated as

$$C_{out} = \log_2 (1 + \gamma_{th}) \left(1 - F_{\gamma_{(R-k+1:R)}}(\gamma_{th}) \right). \quad (44)$$

We have derived the asymptotic distribution of the maximum of R NCCS RVs with one d.o.f. for the cases of a). i.n.i.d. b). i.i.d. RVs. Further, we have derived the k -th order statistics of NCCS RVs and presented stochastic ordering results. The derived asymptotic distributions are used to find the multi-RIS system's outage capacity and average throughput. In the next section, we will see how these asymptotic results serve as approximations in simulations even when R is not tending to infinity.

IV. SIMULATION RESULTS

In the simulations, we consider R RISs, and each RIS takes the number of reflecting elements from a finite set N_1, N_2, N_3 . As per the system model, we can observe that received SNR γ^r at the destination follows an NCCS distribution with one d.o.f with the parameters $\lambda_r = \left(\frac{N_r \pi}{4}\right)^2$ and $\sigma_r^2 = N_r \left(1 - \frac{\pi^2}{16}\right)$. In the simulations, we consider R i.n.i.d NCCS RVs with one d.o.f with

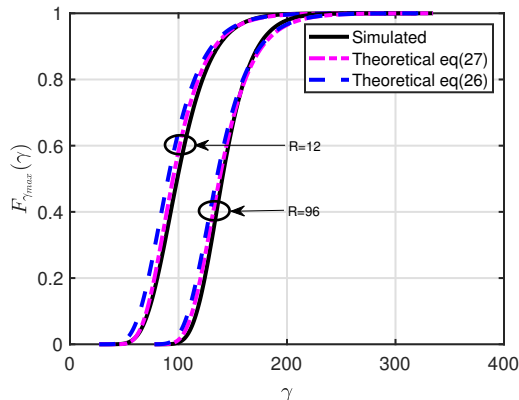


Fig. 2: CDF of γ_{max} (equations (26), (27)) for i.n.i.d. RVs with $N_1 = 10$, $N_2 = 8$, and $N_3 = 6$ the CDF given in (10). Here we consider R_i RVs with parameters (λ_i, σ_i) where $i \in \{1, \dots, P\}$ such that $\sum_{i=1}^P R_i = R$. We compare the theoretical and empirical CDFs of maximum order statistics. In Fig. 2, we compare equation (26) with equation (27) and simulated CDF. Note, for finite R our derived equation (27) will always be close to simulated CDF. Hence, for all other figures, we compare the simulated CDF with the derived equation (27) when we discuss them.

A. i.n.i.d. results

In Fig. 3, we present the CDFs of maximum order statistics for the values of $R = 12, 24$, and 48 with the following number of reflecting elements $N_1 = 10$, $N_2 = 8$, and $N_3 = 6$ with $R_1 = \frac{R}{3}$, $R_2 = \frac{R}{3}$, and $R_3 = \frac{R}{3}$. We assume $\epsilon = \sqrt{\frac{\sigma}{\lambda}}$ as the constant throughout the simulations. Fig. 4 presents the results assuming $N_1 = 15$, $N_2 = 13$, and $N_3 = 11$ as the number of reflecting elements. In Fig. 4 we consider the values $R = 12, 24$, and 48 with $R_1 = \frac{R}{2}$, $R_2 = \frac{R}{4}$, and $R_3 = \frac{R}{4}$. In Fig. 3 and Fig. 4, the solid line presents the results of simulated CDF, and the dashed line presents the results of the theoretical CDF of maximum order statistics. Here, we can observe that, in both cases (Fig. 3,4), simulated and theoretical values are close to each other, and we can also observe that as the number of RVs (R) increases, we are getting better

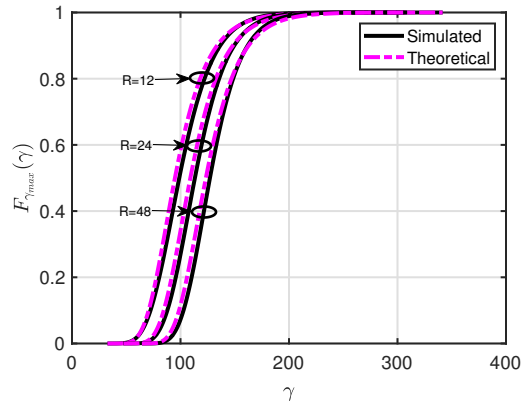


Fig. 3: CDF of γ_{max} for i.n.i.d. RVs with $N_1 = 10$, $N_2 = 8$, and $N_3 = 6$

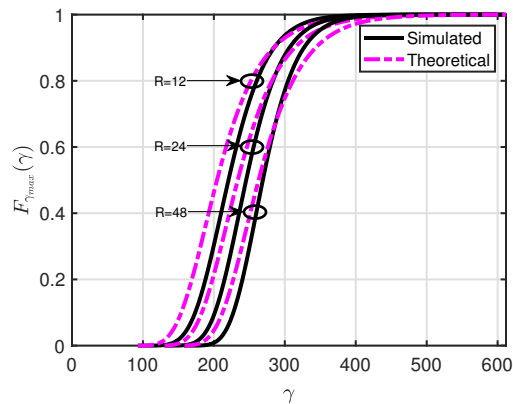


Fig. 4: CDF of γ_{max} for i.n.i.d. RVs with $N_1 = 15$, $N_2 = 13$, and $N_3 = 11$

results. Also, from the simulations, we can observe that even for small values of R , the derived results are in good agreement with the simulated results. The results of Fig. 3 are better than Fig. 4 as the approximation of the Marcum-Q function in (15) is good for lower values of N .

B. i.i.d. results

In this section, we validate the results of the section-III corollary 1.1. Here we consider the equal number of reflecting elements in each RIS leading to i.i.d. NCCS RVs with one d.o.f. We assume that all RISs will have the same number of reflecting elements, i.e., N , and we consider R i.i.d. NCCS random variables. Fig. 5 presents the results assuming $N = 10$ as the number of reflecting elements for all RISs. In Fig. 5 we consider $R = 12, 24$, and 48 respectively with $N_1 = 10; 1 \leq r \leq R$. Fig. 6 assumes $N = 12$ as the number of reflecting elements for all RISs. In Fig. 6 we consider $R = 12, 24$, and 48 respectively with $N_1 = 12; 1 \leq r \leq R$. Here also, we

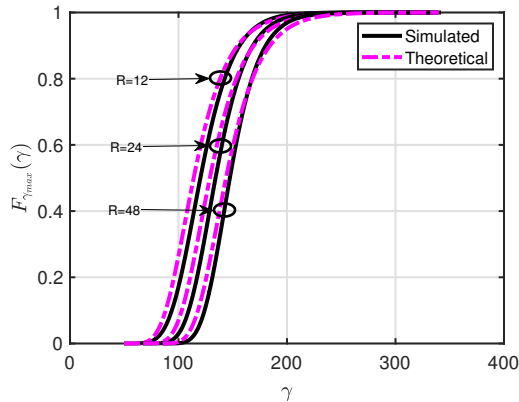


Fig. 5: CDF of γ_{max} for i.i.d. RVs with $N = 10$

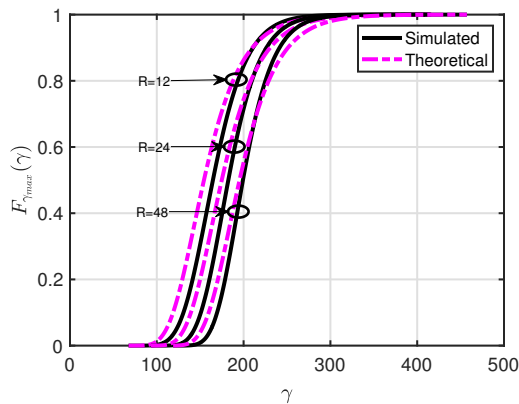


Fig. 6: CDF of γ_{max} for i.i.d. RVs with $N = 12$

can observe that theoretical and empirical CDFs for different values of R are in good agreement, and there is improvement in the results with an increase in R . Note all prior work assumes the same number of reflecting elements for all RISs while using EVT to compute the maximum. In [34], the authors assumed i.i.d. NCCS RVs and expressed the limiting distribution as Gumbel CDF. We derived the identical results as a special case and presented them in corollary 1.1.

C. Results for k -th maximum

Here we present the results of the simulation experiments in the case of k -th maximum order statistics for both i.n.i.d. and i.i.d. random variables. Here we validate the results of section-III corollary 1.2. Fig. 7 presents the results assuming $N_1 = 12$, $N_2 = 10$, and $N_3 = 8$ where the results are plotted for different values of k . Results for i.i.d. case are presented in Fig. 8 assuming $N = 10$, for different values of k . In both cases, we have assumed the number of RVs

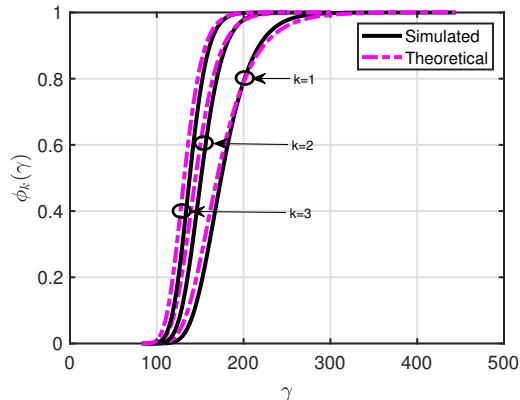


Fig. 7: CDF of $\phi_k(\gamma)$ for i.n.i.d. RVs with $N_1 = 12$, $N_2 = 10$, and $N_3 = 8$

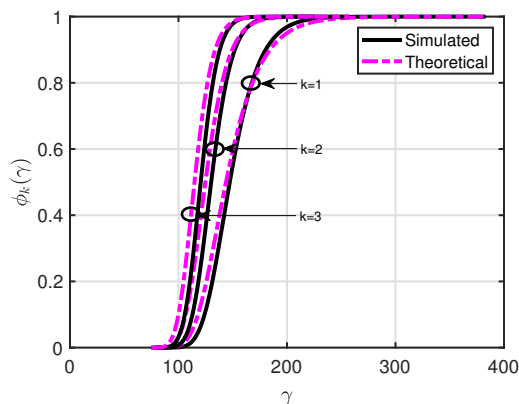


Fig. 8: CDF of $\phi_k(\gamma)$ for i.i.d. RVs with $N = 10$

to be $R = 96$, and we can observe that first-order statistics are better than second and third-order statistics.

D. Results for Stochastic ordering

Fig. 9 presents the stochastic ordering results. Simulated and theoretical CDFs for maximum order statistics for values of $\gamma_a=10\text{dB}$ and 30dB , respectively, are plotted considering i.n.i.d. NCCS RVs with one d.o.f. The results in Fig. 9 are plotted considering the large number of reflecting elements on each RIS ($N_1 = 60$, $N_2 = 55$, and $N_3 = 50$). As the number of reflecting elements increases on each RIS, we can observe that λ_r, σ_r^2 of γ^r increases as $(\frac{N_r\pi}{4})^2, N_r(1 - \frac{\pi^2}{16})$, respectively as shown in the system model (for $N = 60$, $\lambda = 2220.7$ and $\sigma = 4.79$). As the parameter λ grows much faster than σ for each γ^r , we can observe that the CDF of γ_{max} becomes steeper, as shown in Fig. 9. The results in Fig. 9 also show that even for

a large number of reflecting elements, simulated and theoretical CDFs are in good agreement. Further, stochastic ordering has not been characterized before for i.n.i.d. RVs.

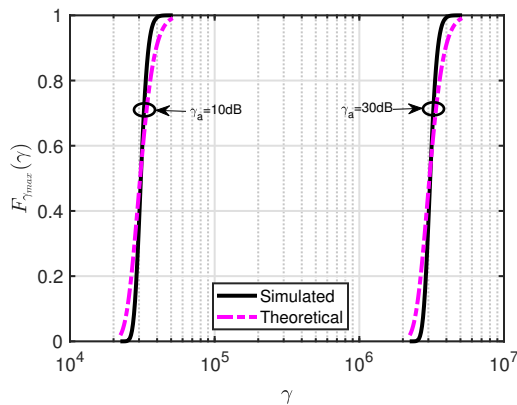


Fig. 9: CDF of $\phi_1(\gamma)$ for different γ_a with $N_1 = 60$, $N_2 = 55$, and $N_3 = 50$

E. Results for Outage capacity and Average throughput

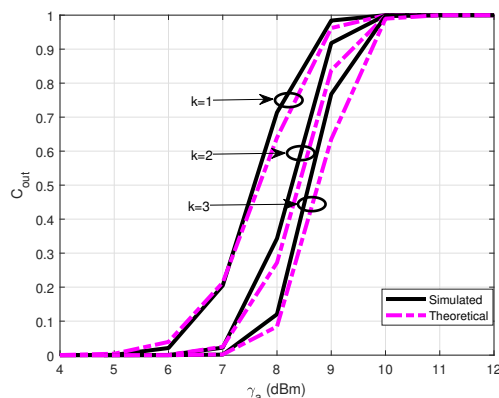


Fig. 10: Outage Capacity Vs SNR with $\gamma_{th}=0$ dB

Here, we present the results for the outage capacity expression derived in (44) for a multi-RIS communication system. Fig. 10 presents the results of outage capacity for different values of k . The results are presented considering i.n.i.d. NCCS RVs with $N_1 = 12$, $N_2 = 10$, and $N_3 = 8$ for a threshold of $\gamma_{th}=0$ dB. We can observe that maximum order statistics, i.e., $k = 1$, achieve the best performance. Next, Fig. 11 compares the outage probability of a multi-RIS system for different numbers of reflecting elements (N_1, N_2, N_3). We can observe that CDF expression of k -th order statistics involves the terms $\tilde{\lambda}$ and $\tilde{\sigma}$, which in turn depends on the

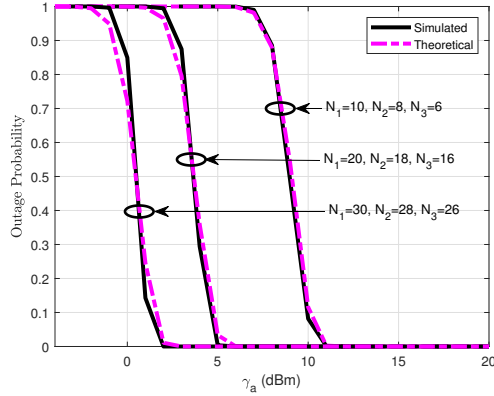


Fig. 11: Outage Probability Vs SNR with $\gamma_{th}=0$ dB for different N

number of reflecting elements as $\lambda_r = \left(\frac{N_r \pi}{4}\right)^2$ and $\sigma_r^2 = N_r \left(1 - \frac{\pi^2}{16}\right)$. Hence, it can be clearly seen that the number of reflecting elements plays a crucial role on the system performance. In Fig. 11, outage probability is plotted for different numbers of reflecting elements. It can be clearly observed that as the number of reflecting elements is increased, outage probability decreases. Fig. 12 shows the average throughput for different values of γ_a and R for maximum

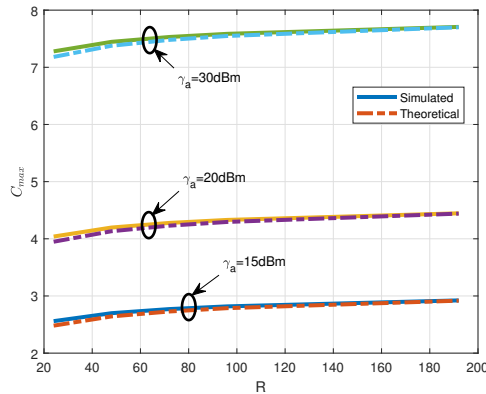


Fig. 12: Average throughput Vs R

order statistics. We have evaluated the theoretical average throughput with pdf expression in (42). Here we have used $N_1 = 12$, $N_2 = 8$, and $N_3 = 4$ for simulation experiments.

Next, Fig. 13 presents the results of average throughput Vs SNR considering different numbers of reflecting elements. We can also observe from the plots that as the number of reflecting elements increases average throughput of the system is also increasing. We have used $R = 24$ for this simulation, and the number of reflecting elements used are $(N_1 = 10, N_2 = 8, N_3 = 6)$,

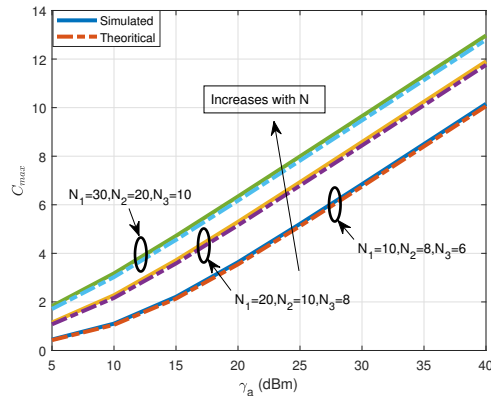


Fig. 13: Average throughput of a multi-RIS system for different N

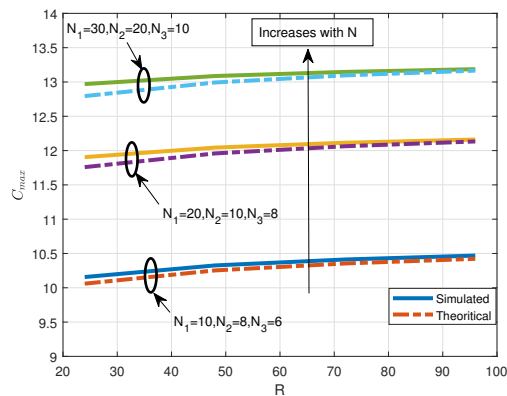


Fig. 14: Average throughput of a multi-RIS system for different N and R

($N_1 = 20, N_2 = 10, N_3 = 8$), and ($N_1 = 30, N_2 = 20, N_3 = 10$).

Fig. 14 compares the average throughput of a multi-RIS system for different R and different numbers of reflecting elements. We know that as the number of RVs (R) increases, the simulated and theoretical average throughputs should converge asymptotically. We can observe that convergence happens even with finite values of R . We can observe that the average throughput of the RIS-aided system can be improved with more reflecting elements on each RIS. Fig. 14 presents the results of average throughput using the reflecting elements as ($N_1 = 10, N_2 = 8, N_3 = 6$), ($N_1 = 20, N_2 = 10, N_3 = 8$), and ($N_1 = 30, N_2 = 20, N_3 = 10$).

V. CONCLUSIONS

In this paper, we analyzed the performance of a multi-RIS (R RIS) system where the RISs can have a different number of reflecting elements. Assuming the highest SNR link gets selected

for communication, we derived the asymptotic distribution of normalized maximum SNR RV. We further derived k -th order statistics of i.n.i.d. SNR RVs to deal with scenarios where one is interested in selecting the k -th best link. Using our results, we provided outage probability and average throughput expressions for a multi-RIS system. The simulations showed that the derived asymptotic distribution is in good agreement with the exact distribution, even for moderate values of R .

REFERENCES

- [1] Q. Wu and R. Zhang, "Intelligent reflecting surface enhanced wireless network via joint active and passive beamforming," *IEEE transactions on wireless communications*, vol. 18, no. 11, pp. 5394–5409, 2019.
- [2] Q. Wu and R. Zhang, "Beamforming optimization for wireless network aided by intelligent reflecting surface with discrete phase shifts," *IEEE Transactions on Communications*, vol. 68, no. 3, pp. 1838–1851, 2019.
- [3] S. Abeywickrama, R. Zhang, Q. Wu, and C. Yuen, "Intelligent reflecting surface: Practical phase shift model and beamforming optimization," *IEEE Transactions on Communications*, vol. 68, no. 9, pp. 5849–5863, 2020.
- [4] C. Pan, H. Ren, K. Wang, W. Xu, M. Elkashlan, A. Nallanathan, and L. Hanzo, "Multicell mimo communications relying on intelligent reflecting surfaces," *IEEE Transactions on Wireless Communications*, vol. 19, no. 8, pp. 5218–5233, 2020.
- [5] C. Pan, H. Ren, K. Wang, M. Elkashlan, A. Nallanathan, J. Wang, and L. Hanzo, "Intelligent reflecting surface aided MIMO broadcasting for simultaneous wireless information and power transfer," *IEEE Journal on Selected Areas in Communications*, vol. 38, no. 8, pp. 1719–1734, 2020.
- [6] S. Zhang and R. Zhang, "Capacity characterization for intelligent reflecting surface aided MIMO communication," *IEEE Journal on Selected Areas in Communications*, vol. 38, no. 8, pp. 1823–1838, 2020.
- [7] G. Zhou, C. Pan, H. Ren, K. Wang, M. Di Renzo, and A. Nallanathan, "Robust beamforming design for intelligent reflecting surface aided MISO communication systems," *IEEE Wireless Communications Letters*, vol. 9, no. 10, pp. 1658–1662, 2020.
- [8] B. Di, H. Zhang, L. Song, Y. Li, Z. Han, and H. V. Poor, "Hybrid beamforming for reconfigurable intelligent surface based multi-user communications: Achievable rates with limited discrete phase shifts," *IEEE Journal on Selected Areas in Communications*, vol. 38, no. 8, pp. 1809–1822, 2020.
- [9] Q. Wu and R. Zhang, "Joint active and passive beamforming optimization for intelligent reflecting surface assisted SWIPT under QoS constraints," *IEEE Journal on Selected Areas in Communications*, vol. 38, no. 8, pp. 1735–1748, 2020.
- [10] C. Huang, R. Mo, and C. Yuen, "Reconfigurable intelligent surface assisted multiuser MISO systems exploiting deep reinforcement learning," *IEEE Journal on Selected Areas in Communications*, vol. 38, no. 8, pp. 1839–1850, 2020.
- [11] S. Li, B. Duo, X. Yuan, Y.-C. Liang, and M. Di Renzo, "Reconfigurable intelligent surface assisted UAV communication: Joint trajectory design and passive beamforming," *IEEE Wireless Communications Letters*, vol. 9, no. 5, pp. 716–720, 2020.
- [12] B. Zheng, Q. Wu, and R. Zhang, "Intelligent reflecting surface-assisted multiple access with user pairing: NOMA or OMA?" *IEEE Communications Letters*, vol. 24, no. 4, pp. 753–757, 2020.
- [13] S. Gopi, S. Kalyani, and L. Hanzo, "Intelligent reflecting surface assisted beam index-modulation for millimeter wave communication," *IEEE Transactions on Wireless Communications*, vol. 20, no. 2, pp. 983–996, 2020.
- [14] A. Taha, M. Alrabeiah, and A. Alkhateeb, "Enabling large intelligent surfaces with compressive sensing and deep learning," *IEEE access*, vol. 9, pp. 44 304–44 321, 2021.

- [15] H. Yang, Z. Xiong, J. Zhao, D. Niyato, L. Xiao, and Q. Wu, "Deep reinforcement learning-based intelligent reflecting surface for secure wireless communications," *IEEE Transactions on Wireless Communications*, vol. 20, no. 1, pp. 375–388, 2020.
- [16] M. Charishma, A. Subhash, S. Shekhar, and S. Kalyani, "Outage probability expressions for an IRS-assisted system with and without source-destination link for the case of quantized phase shifts in κ - μ fading," *IEEE Transactions on Communications*, vol. 70, no. 1, pp. 101–117, 2021.
- [17] A. Subhash, A. Kammoun, A. Elzanaty, S. Kalyani, Y. H. Al-Badarneh, and M.-S. Alouini, "Max-Min SINR optimization for RIS-aided uplink communications with green constraints," *IEEE Wireless Communications Letters*, 2023.
- [18] A. Subhash, A. Kammoun, A. Elzanaty, S. Kalyani, Y. H. Al-Badarneh, and M.-S. Alouini, "Optimal phase shift design for fair allocation in RIS aided uplink network using statistical CSI," *IEEE Journal on Selected Areas in Communications*, 2023.
- [19] S. Shekhar, A. Subhash, T. Kella, and S. Kalyani, "Instantaneous channel oblivious phase shift design for an IRS-assisted SIMO system with quantized phase shift," *arXiv preprint arXiv:2211.03317*, 2022.
- [20] E. Basar, M. Di Renzo, J. De Rosny, M. Debbah, M.-S. Alouini, and R. Zhang, "Wireless communications through reconfigurable intelligent surfaces," *IEEE access*, vol. 7, pp. 116 753–116 773, 2019.
- [21] L. Yang, Y. Yang, M. O. Hasna, and M.-S. Alouini, "Coverage, probability of SNR gain, and DOR analysis of RIS-aided communication systems," *IEEE Wireless Communications Letters*, vol. 9, no. 8, pp. 1268–1272, 2020.
- [22] T. N. Do, G. Kaddoum, T. L. Nguyen, D. B. Da Costa, and Z. J. Haas, "Multi-RIS-aided wireless systems: Statistical characterization and performance analysis," *IEEE Transactions on Communications*, vol. 69, no. 12, pp. 8641–8658, 2021.
- [23] V.-D. Phan, B. C. Nguyen, T. M. Hoang, T. N. Nguyen, P. T. Tran, B. V. Minh, and M. Voznak, "Performance of cooperative communication system with multiple reconfigurable intelligent surfaces over Nakagami-m fading channels," *IEEE Access*, vol. 10, pp. 9806–9816, 2022.
- [24] Z. Xie, W. Yi, X. Wu, Y. Liu, and A. Nallanathan, "Downlink multi-RIS aided transmission in backhaul limited networks," *IEEE Wireless Communications Letters*, vol. 11, no. 7, pp. 1458–1462, 2022.
- [25] P. T. Tran, B. C. Nguyen, T. M. Hoang, X. H. Le *et al.*, "Exploiting multiple RISs and direct link for performance enhancement of wireless systems with hardware impairments," *IEEE Transactions on Communications*, vol. 70, no. 8, pp. 5599–5611, 2022.
- [26] P. T. Tran, B. C. Nguyen, T. M. Hoang, N. Van Vinh *et al.*, "Combining multi-RIS and relay for performance improvement of multi-user NOMA systems," *Computer Networks*, vol. 217, p. 109353, 2022.
- [27] E. K. Agbogle, I. Trigui, K. Humadi, W. Ajib, and W.-P. Zhu, "Adaptive coordinated direct and multi-RIS transmissions for ultrareliable terahertz systems," *IEEE Transactions on Vehicular Technology*, 2023.
- [28] B. C. Nguyen, Q.-N. Van, L. T. Dung, T. M. Hoang, N. V. Vinh, and G. T. Luu, "Secrecy performance of multi-RIS-assisted wireless systems," *Mobile Networks and Applications*, pp. 1–14, 2023.
- [29] B. C. Nguyen, N. T. Xuan, H. T. Manh, H. L. T. Thanh, and P. T. Hiep, "Performance analysis for multi-RIS UAV NOMA mmwave communication systems," *Wireless Networks*, vol. 29, no. 2, pp. 761–773, 2023.
- [30] Y. Fang, S. Atapattu, H. Inaltekin, and J. Evans, "Optimum reconfigurable intelligent surface selection for wireless networks," *IEEE Transactions on Communications*, vol. 70, no. 9, pp. 6241–6258, 2022.
- [31] M. Aldababsa, A. M. Salhab, A. A. Nasir, M. H. Samuh, and D. B. da Costa, "Multiple RISs-aided networks: Performance analysis and optimization," *IEEE Transactions on Vehicular Technology*, 2023.
- [32] R. Hindustani, D. Dixit, S. Sharma, and V. Bhatia, "Outage probability of multiple-IRS-assisted SISO wireless communications over rician fading," *Physical Communication*, vol. 59, p. 102102, 2023.

- [33] D. T. Tam, N. Van Vinh, and B. C. Nguyen, "Improving the performance of multi-IRS aided millimeter-wave communication systems by transmit antenna selection," *Physical Communication*, vol. 56, p. 101957, 2023.
- [34] L. Yang, Y. Yang, D. B. da Costa, and I. Trigui, "Outage probability and capacity scaling law of multiple RIS-aided networks," *IEEE Wireless Communications Letters*, vol. 10, no. 2, pp. 256–260, 2020.
- [35] D. Park and S. Y. Park, "Performance analysis of multiuser diversity under transmit antenna correlation," *IEEE transactions on communications*, vol. 56, no. 4, pp. 666–674, 2008.
- [36] W. Seo, H. Song, J. Lee, and D. Hong, "A new asymptotic analysis of throughput enhancement from selection diversity using a high SNR approach in multiuser systems," *IEEE Transactions on Wireless Communications*, vol. 8, no. 1, pp. 55–59, 2009.
- [37] M. Xia and S. Aissa, "Spectrum-sharing multi-hop cooperative relaying: Performance analysis using extreme value theory," *IEEE transactions on wireless communications*, vol. 13, no. 1, pp. 234–245, 2013.
- [38] F. Haider, C.-X. Wang, H. Haas, E. Hepsaydir, X. Ge, and D. Yuan, "Spectral and energy efficiency analysis for cognitive radio networks," *IEEE Transactions on Wireless Communications*, vol. 14, no. 6, pp. 2969–2980, 2015.
- [39] C.-F. Liu, M. Bennis, M. Debbah, and H. V. Poor, "Dynamic task offloading and resource allocation for ultra-reliable low-latency edge computing," *IEEE Transactions on Communications*, vol. 67, no. 6, pp. 4132–4150, 2019.
- [40] S. Samarakoon, M. Bennis, W. Saad, and M. Debbah, "Distributed federated learning for ultra-reliable low-latency vehicular communications," *IEEE Transactions on Communications*, vol. 68, no. 2, pp. 1146–1159, 2019.
- [41] A. Subhash, M. Srinivasan, S. Kalyani, and L. Hanzo, "Transmit power policy and ergodic multicast rate analysis of cognitive radio networks in generalized fading," *IEEE Transactions on Communications*, vol. 68, no. 6, pp. 3311–3325, 2020.
- [42] S. Kalyani and R. Karthik, "The asymptotic distribution of maxima of independent and identically distributed sums of correlated or non-identical gamma random variables and its applications," *IEEE transactions on communications*, vol. 60, no. 9, pp. 2747–2758, 2012.
- [43] A. Subhash, M. Srinivasan, and S. Kalyani, "Asymptotic maximum order statistic for SIR in $\kappa - \mu$ shadowed fading," *IEEE Transactions on Communications*, vol. 67, no. 9, pp. 6512–6526, 2019.
- [44] D. Mejlzer and I. Weissman, "On some results of NV smirnov concerning limit distributions for variational series," *The Annals of Mathematical Statistics*, vol. 40, no. 2, pp. 480–491, 1969.
- [45] H. Barakat, E. Nigm, and M. Al-Awady, "Limit theorems for random maximum of independent and non-identically distributed random vectors," *Statistics*, vol. 47, no. 3, pp. 546–557, 2013.
- [46] A. Subhash and S. Kalyani, "Cooperative relaying in a SWIPT network: Asymptotic analysis using extreme value theory for non-identically distributed RVs," *IEEE Transactions on Communications*, vol. 69, no. 7, pp. 4360–4372, 2021.
- [47] A. Subhash, S. Kalyani, Y. H. Al-Badarneh, and M.-S. Alouini, "On the asymptotic performance analysis of the k-th best link selection over non-identical non-central chi-square fading channels," *IEEE Transactions on Communications*, vol. 70, no. 11, pp. 7191–7206, 2022.
- [48] I. Yildirim, A. Uyrus, and E. Basar, "Modeling and analysis of reconfigurable intelligent surfaces for indoor and outdoor applications in future wireless networks," *IEEE transactions on communications*, vol. 69, no. 2, pp. 1290–1301, 2020.
- [49] D. L. Galappaththige, D. Kudathanthirige, and G. A. A. Baduge, "Performance analysis of distributed intelligent reflective surfaces for wireless communications," *arXiv preprint arXiv:2010.12543*, 2020.
- [50] A. F. Molisch, *Wireless communications*. John Wiley & Sons, 2012.
- [51] L. Haan and A. Ferreira, *Extreme value theory: an introduction*. Springer, 2006, vol. 3.
- [52] H. A. David and H. N. Nagaraja, "Order Statistics," *Encyclopedia of Statistical Sciences*, 2003.

- [53] H. Barakat, "Limit theorems for bivariate extremes of non-identically distributed random variables," *Applicationes Mathematicae*, vol. 4, no. 29, pp. 371–386, 2002.
- [54] E. W. Weisstein, *Incomplete Gamma Function: From MathWorld—A Wolfram Web Resource*, accessed October 01, 2020). [Online]. Available: <https://mathworld.wolfram.com/IncompleteGammaFunction.html>
- [55] E. W. Weisstein, *Gamma Function: From MathWorld—A Wolfram Web Resource*, accessed October 01, 2020). [Online]. Available: <https://mathworld.wolfram.com/GammaFunction.html>